Silicon (2019) 11:2233–2239
DOI 10.1007/s12633-015-9402-8

ORIGINAL PAPER

Preparation, Mechanical and Antimicrobial Properties of SiO_2/ Poly(butylene adipate-co-terephthalate) Films for Active Food Packaging

R. Venkatesan[1] · **N. Rajeswari**[1]

Received: 24 September 2015 / Accepted: 28 December 2015 / Published online: 20 April 2016

Abstract In this study, transparent thin film of SiO_2 nanoparticles (NPs) filled poly(butylene adipate-co-terephthalate) (PBAT) composites were prepared by a solvent casting method, with chloroform ($CHCl_3$) as a solvent. This paper is focused on studying the mechanical and antimicrobial activity of SiO_2 NPs in PBAT films. The morphological characteristics were studied by using FTIR and XRD spectroscopy. SEM, HRTEM investigations confirm the homogeneous dispersion of SiO_2 NPs in the PBAT matrix. The tensile strength increases significantly by introducing the SiO_2 NPs of (5 wt%) into the PBAT matrix, in which PBAT/SiO_2 films have greater tensile strength (58.01 MPa) when compared to the PBAT polymer (33.75 MPa). In this study we found that PBAT/SiO_2 had increased mechanical properties, increased contact angle and decreased oxygen permeability, and moisture uptake of the nanocomposite film. Further antimicrobial activity by the well diffusion assay method was followed against S. aureus, and E. coli which were found to have good inhibition effect.

Keywords Nano-composite · Poly (butylene adipate-co-terephthalate) · SiO_2 nanoparticles · Mechanical strength · Antimicrobial activity

✉ R. Venkatesan
mahavenki_1619@yahoo.com; rajavenki101@gmail.com

[1] Department of Printing Technology, College of Engineering Guindy, Anna University, Chennai 600 025, Tamil Nadu, India

1 Introduction

Nanocomposites (NCs)' have been used in automotive, packaging, building and agricultural materials [1]. Various polymeric nanocomposites have been extensively studied, including polyamide, epoxy, polyester, polystyrene and polypropylene [2]. In recent years, to solve the waste disposal problem of plastic materials, biodegradable polymers have become an important trend [3]. Adding nano-fillers into the biodegradable polymers can increase mechanical, thermal, dimensional and barrier properties of the composite films.

Nano-silica (SiO_2) filled polymer matrix composites have attracted significant attention in the past few years. The mechanical and thermal properties of SiO_2-filled polymer matrix composite materials have been reported [4–6]. Studies on SiO_2 dispersion in polymer matrices such as poly(methyl methacrylate) [7, 8] high density polyethylene [9] and poly(ethylene oxide) [10] have been carried out. PBAT is a large-scale polymer product used extensively to produce fibres, films and packaging materials due to its good mechanical and optical properties [11, 12] resistance to creep fracture and resistance to fatigue and wear.

The development of composite PBAT has led to materials with additional functional properties such as antibacterial activity [13, 14]. The high performance, biodegradable PBS/PBAT composite film exhibited enhancement in tensile strength and elongation at break. This blended composite indicates that a good compatibility is achieved between the polymers [15]. The PBS/PBAT composites blended with organoclay film gave an improvement in mechanical

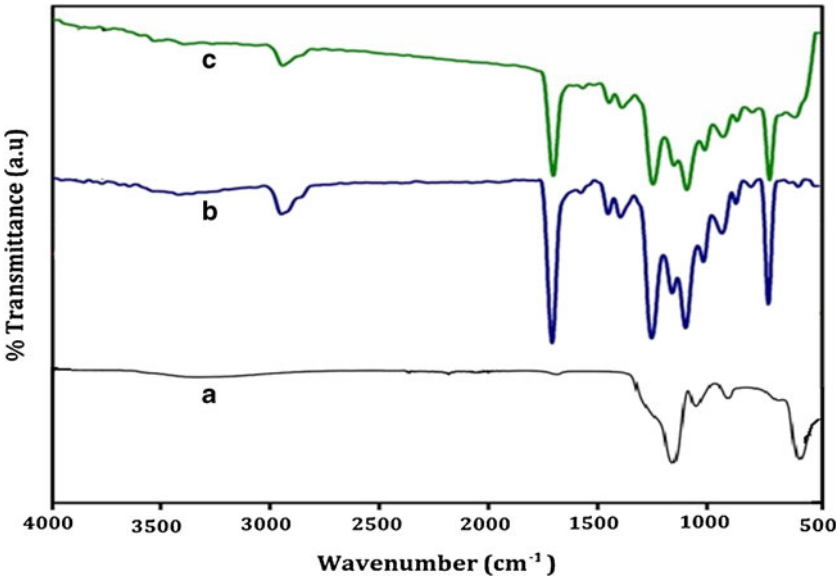

Fig. 1 FT-IR spectra of **a** SiO_2 NPs, **b** PBAT, **c** PBAT/ SiO_2 nanocomposite film

strength [16]. The PBAT-PVOH/SiO_2 NCs films prepared by solvent casting have excellent mechanical and antimicrobial activity [17].

The NCs of biodegradable PBAT and layered silicates have been prepared using a melt intercalation method. Based on the results PBAT/Na^+MMT NCs exhibited a greater weight loss than did control PBAT, NCs with modified clay C30B which indicated that the hydrophilic environment of the Na^+MMT supported the biodegradation of PBAT [18]. PBAT with montmorillonite (MMT) (C30B, C20A and B109) gave improved degradation, thermal stability and mechanical properties of PBAT based NCs. PBAT and layered silicates (3 wt%, PBAT/ODA-M) composite materials showed lower tensile modulus [19]. MWCNTs have been functionalized and incorporated in PBAT based composites by using a simple method [20].

The aim of this study is to prepare NCs by blending SiO_2 in a PBAT polymer matrix. The SiO_2 NPs are prepared using the sol-gel method, a fast, simple and low cost method. The prepared nanocomposite films were analysed by FT-IR, XRD, SEM and HRTEM. The antimicrobial property of the prepared polymer NCs films was evaluated against two food pathogenic bacteria, *S. aureus* and *E. coli*, by using the agar disk diffusion method.

2 Experimental Section

2.1 Materials

The PBAT (Ecoflex) with melt flow index (MFI) 3.3–6.6 g/10 min (at 190 ºC; 2.16 kg) and density 1.25–1.27 g/cm^3, and melting point 110–115 °C was supplied by M/s BASF Japan Ltd. (TEOS) tetraethoxysilane was purchased from Sigma-Aldrich, India. The test strains, *E.coli* MTCC 1303, *S.aureus*, ATCC 6538 were procured from IMTECH, Chandigarh. All experimental materials, chemicals and solvents were obtained from SRL, India and Sigma Aldrich, India.

2.2 Synthesis of SiO_2 Nanoparticles

Nano-crystalline SiO_2 was synthesized by the sol-gel method using tetraethoxysilane (TEOS) as a source of silicon. 7.4 ml of TEOS was added to 80 ml of methanol and the mixture was stirred vigorously at 150 °C and stirred for a further 30 minutes. A white color powder was obtained and was heated in a tubular furnace at 300 ºC for 1 hour to get the SiO_2 powder with particle size 35 nm.

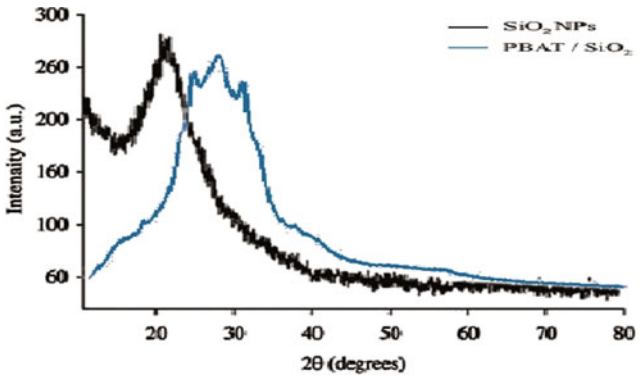

Fig. 2 XRD patterns of the PBAT/SiO_2 nanocomposite film

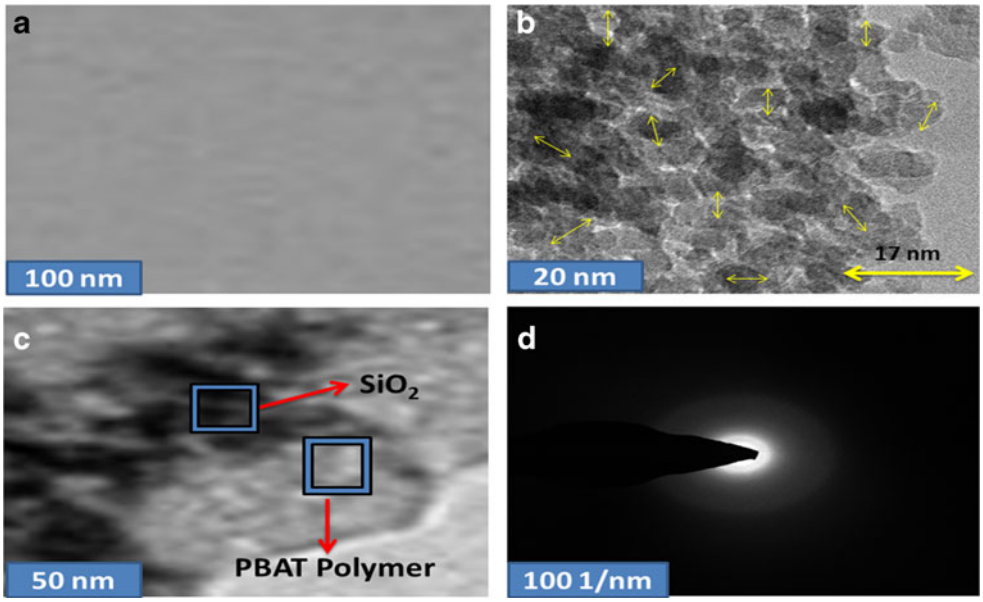

Fig. 3 HRTEM images of **a** PBAT, **b** SiO_2 NPs, **c** PBAT/SiO_2, **d** SAED pattern of PBAT/SiO_2 nanocomposite film

2.3 Preparation PBAT/SiO_2Nanocomposite Films

Approximately, 2.0 g of PBAT polymer granules were dissolved in 98 ml of chloroform with constant stirring until a clear solution was obtained. Instantaneously, the (5 wt%) SiO_2 nanoparticles were dispersed in the polymer solution. The solution were cast into a petri dish [17, 21–24] and dried in an oven for 48 hrs at 40 °C. Finally, the resulting films were dried under vacuum for 48 hrs to remove the residual solvent. Homogeneous films of 0.05–0.1 mm thickness were obtained.

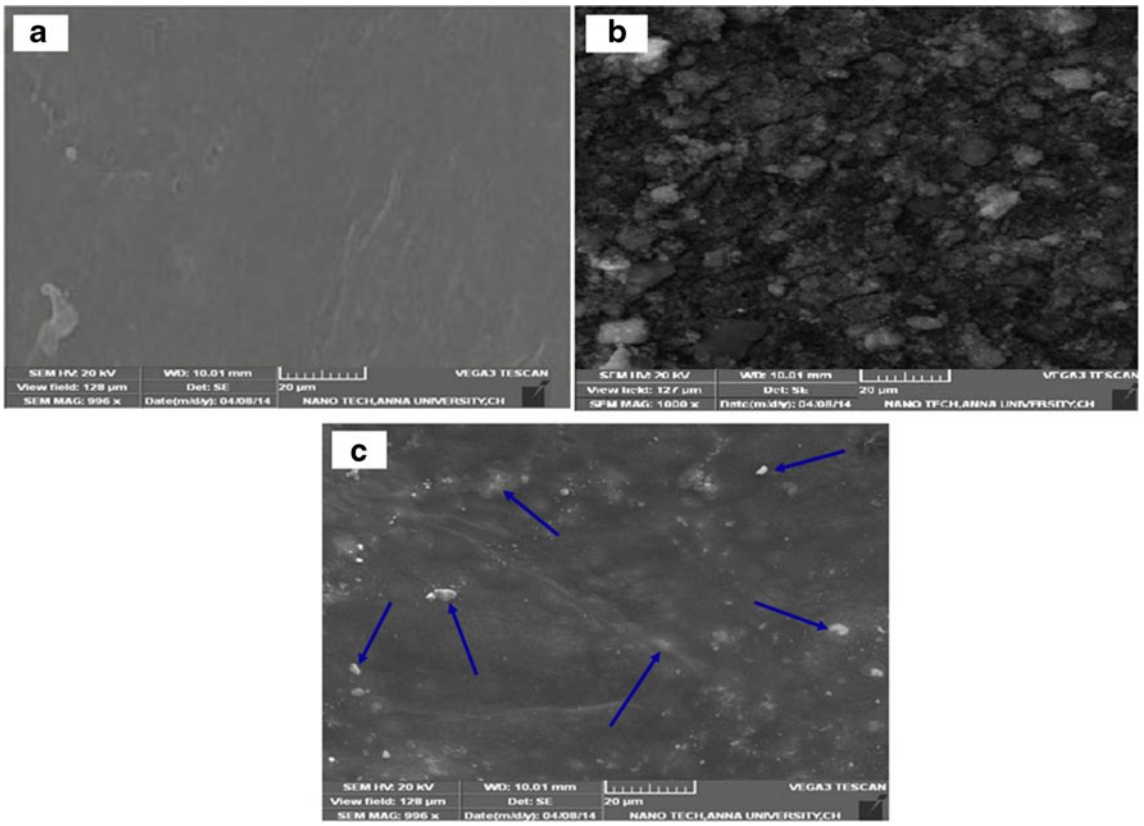

Fig. 4 SEM images of **a** PBAT, **b** SiO_2 NPs **c** PBAT nanocomposite film

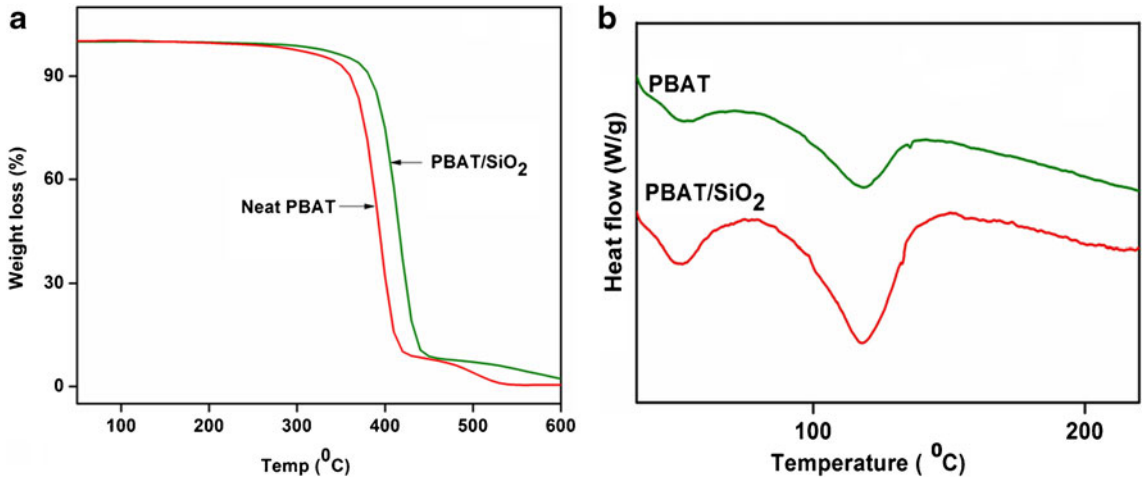

Fig. 5 **a** TGA **b** DSC thermograms of PBAT and PBAT/SiO_2 film

2.4 Characterization

The FT-IR spectra of the samples as pieces of the cast films were examined in the frequency range of 400–4000 cm^{-1} at a resolution of 4 cm^{-1} using a (Perkin Elmer spectrophotometer RX1). XRD analysis of the NC film was performed at room temperature with an (Rigaku) analytical diffractometer using Cu, Ka radiation (MiniFlex II-C). High resolution transmission electron microscopy (HRTEM) was carried out on a TECNAI-G2 (model T-30) at an accelerating voltage of 300 kV. Scanning electron microscopy (SEM) measurements were performed on a HITACHI S-3000H scanning electron microscope. A piece of film was fixed in the surface of the double-sided adhesive tape and the film was sputtered with gold prior to SEM observation. The calorimetric analysis of the nanocomposites was performed on a (SII, Nanotech, DSC-6220) differential scanning calorimeter (DSC) at a heating rate of 10 °C min^{-1} under nitrogen atmosphere. Thermal gravimetric analysis (TA Instruments Q50) was used to study the thermal stability of PBAT and NCs film. 10 mg samples were heated from room temperature to 750 °C under a continuous flow of nitrogen (20 mL/min). The mechanical strength was analyzed using a universal testing machine (UTM, H10KS, Tinius Olsen) according to the ASTM D 638-03 method. Barrier properties (OTR) of the PBAT/SiO_2 nanocomposite films were characterized by (Noselab ats). The contact angle of NC films was measured by using a Goniometer (GBX Digidrop) at 27 °C. The moisture uptake (MU) of the NC films was determined at RH of 70 % by the method proposed by Yang et al. [25].

2.5 Antimicrobial Activity Test

The antimicrobial activity of NC film was tested by an inhibition zone method (ISO 22196). Food pathogenic bacteria *E.coli* and *S.aureus* were used for the antimicrobial activity study of the NC film. The plates were examined for possible clear zones after incubation at 37 °C for 2 days.

3 Results and Discussion

3.1 FT – IR Analysis

The interactions between polymer and SiO_2 in composites can be identified through an analysis of the FT-IR spectra. The FT-IR spectra of a PBAT film, SiO_2 NPs and PBAT/SiO_2 film are shown in (Fig. 1). In the FT-IR spectrum of pure PBAT, a characteristic vibration band of C=O stretching is observed at 1712 cm^{-1}, those of C-O stretching are found at 1285 and 795 cm^{-1} and that of C-H stretching is observed at 2980 cm^{-1}. The spectra of the PBAT/SiO_2 films clearly exhibit characteristic absorption peaks corresponding to only polymeric groups of pure PBAT. That is, the FT-IR spectra of the NC films show no change or shift

Table 1 Effect of PBAT, SiO_2 loading on tensile strength and elongation at break

Sample	Tensile strength (MPa)	Elongation (%)
PBAT	33.75	600
PBAT/SiO_2	58.01	980

Table 2 Oxygen transmission rate of the neat polymer and nanocomposite measured at 25 °C

Sample	OTR (mL/m^2/day)
PBAT	535.0 ±1.0
PBAT/SiO_2	310.9 ±2.2

Table 3 MU at equilibrium and water CA of PBAT and its nanocomposite film

Sample	Moisture uptake (%)	Water contact angle (°C)
PBAT	41.00	42.50
PBAT/SiO_2	23.60	69.85

in the characteristic peaks of pure PBAT with the addition of SiO_2 particles. The pure PBAT and PBAT/SiO_2 films yielded the same FT-IR spectrum, which means a poor chemical interaction between the PBAT and SiO_2 occurred, or the SiO_2 characteristic peak was overlapped by the PBAT characteristic peak.

3.2 XRD Spectroscopy

The XRD pattern of PBAT/SiO_2 and SiO_2 NPs are shown in Fig. 2. It is obvious that the PBAT polymer is crystalline in nature. It shows the characteristic peaks at $2\theta = 22$, 28 and 35°, which suggest the formation of inter and intra molecular oxygen bonds in the presence of C=O groups in the PBAT polymer. The nano silicon dioxide prepared was highly crystalline in nature. The diffraction peaks were observed at $2\theta = 22°$. From the Scherrer equation the crystalline SiO_2 particle size was found to be 35 nm.

3.3 Surface Morphology of Polymer Nanocomposites (PNC's)

The surface morphology of PBAT and its nanocomposite films was characterized by HRTEM. Figure 3a shows the neat PBAT matrix, and the prepared SiO_2 nanoparticle is shown in Fig. 3b, the particle size is 35 nm. The interaction between the SiO_2 nanoparticles and the PBAT matrix is well revealed from the HRTEM images shown in Fig. 3c. The SiO_2 nanofillers in the PBAT matrix are of spherical shape randomly distributed for 5 wt% of SiO_2 nanocomposite films. The dark spot represents the SiO_2 nanoparticle with polymer background. The selected area electron diffraction (SAED) of the prepared nanocomposite is shown in Fig. 3d. Crystalline and amorphous behavior can be observed from the SAED pattern of the PBAT/SiO_2 nanocomposite film. Diffraction rings of the SAED pattern correspond to the crystal planes of SiO_2 which are exhibited as bright dots, indicating that it consists of SiO2 nanocrystals.

Figure 4 shows the SEM images of neat PBAT and PBAT/SiO_2 film respectively. The neat PBAT film structure is non-homogeneous and uneven, while the SiO_2 incorporated into the PBAT polymer film shows that the SiO_2 nanoparticles are dispersed in the PBAT matrix. In Fig. 4c, the addition of SiO_2 nanomaterials leads to agglomeration in different sizes in the form of spherical shapes, which are due to the SiO_2 nanoparticles present in the nanocomposite film.

3.4 Thermal Properties

Thermal stability of PBAT and PBAT/SiO_2 films is shown in Fig. 5a. In metal oxide incorporation in PBAT film two weight losses are observed, in which the first losses around 240–350 °C is due to water vaporization and the second loss around 400–600 °C is due to degradation of PBAT and SiO_2. These thermal stability changes in the films are due to the presence of SiO_2 nanoparticles in the PBAT polymer matrix. DSC results are shown in Fig. 5b as thermograms for the pure PBAT and PBAT/SiO_2 film. The heating curves show broad endotherms at interval 25–150 °C associated with melting of the PBAT polymer. The PBAT/SiO_2 endotherm is shifted to the higher temperature values. The transition starts at lower temperatures and ends at higher temperatures. Both values are very significantly increased for PBAT/SiO_2 films. As can be seen, it was 127 °C but is 90 % compared to 110 °C and 45 % for the initial PBAT correspondingly.

3.5 Mechanical Properties

The mechanical properties of nanocomposite films are given in Table 1. The tensile strength increases by adding the SiO_2 nanoparticles (5wt %) into the PBAT matrix. PBAT/SiO_2 films have higher tensile strength (58.01 MPa), compared to the pure PBAT (33.75 MPa), because of the good dispersion of SiO_2NPs into the PBAT matrix which prevents

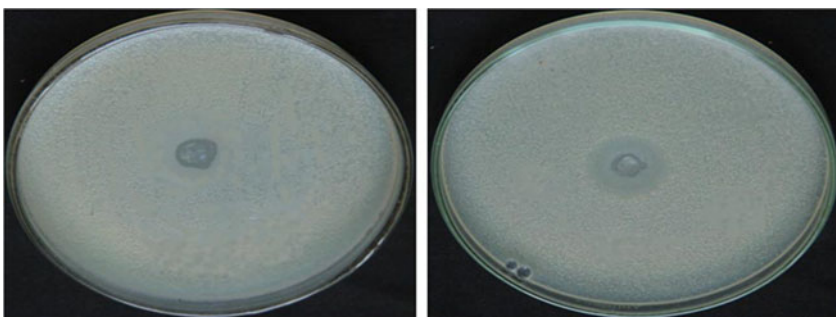

Fig. 6 Antimicrobial test of PBAT and PBAT/SiO_2 against *E.coli*

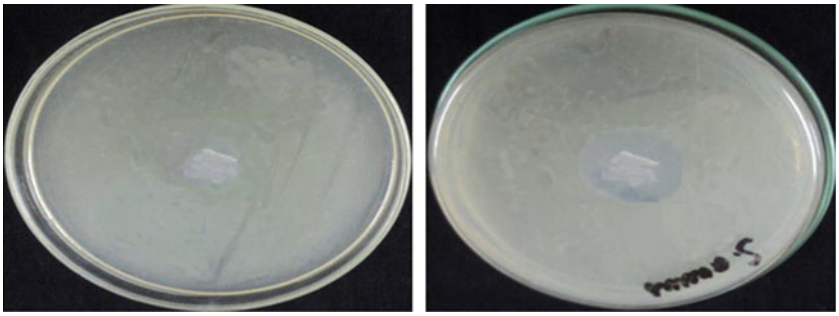

Fig. 7 Antimicrobial test of PBAT and PBAT/SiO_2 against *S.aureus*

material from coagulating and is due to the good interaction between the metal oxide and PBAT. The addition of SiO_2 NPs increased the elongation at break of the composite. This result is attributed to the occurrence of intercalation rather than exfoliation by the decrease of PBAT nanocomposite film having decreased tensile strength and elongation properties when compared to PBAT film.

3.6 Oxygen Transmission Rate (OTR)

The oxygen permeability is one of the most important property in a packaging material to decide its suitability for different applications. For the PBAT, PBAT/SiO_2 films, the OTR values were measured and it is given in Table 2. For the PBAT polymer film, the average OTR value was 535 mL/ m^2 /day. The control PBAT has high oxygen permeability but the decrease in OTR of the NCs film can be attributed to the generation of a tortuous path for the permeation of oxygen molecules in the presence of SiO_2 into the PBAT polymer matrix. The highest value of 535 mL/ m^2 /day was observed for 0 wt% of SiO_2 nanoparticles. Note that the oxygen transmission rate decreased with addition of SiO_2 (5 wt%) nanoparticles. These results are most important and show that on the adding of SiO_2 NPs the value of oxygen transmission rate also decreases.

3.7 Contact Angle & Moisture Uptake Properties

From the water contact angle (CA) (°) wettability of the NCs film surface was determined. For a smooth and flat surface the contact angle decreases as the affinity of the liquid drop increases. Higher contact angle indicates poorer wettability. The contact angle was measured for both pure PBAT and PBAT/SiO_2 NCs films to understand the wetting properties [26]. Hydrophobic surfaces are signified by a contact angle which is above 90° and a lower contact angle represents a more hydrophilic surface. The water contact angle of PBAT/SiO_2 increases with introducing the SiO_2 NPs, as shown in Table 3. The interaction between polymer and SiO_2 nanoparticle decreases the water sensitivity of the nanocomposite. In addition, the surface hydrophobicity of SiO_2 NPs is better than that of the polymer. The effect of SiO_2 NPs on the moisture uptake (MU) of the film is shown in Table 3, it can be seen that the (MU) of the NC's decreases with addition of the SiO_2 NPs.

Table 4 Effect of SiO_2 based antimicrobial films on the inhibition zones

Strain	The inhibition zone (mm)	
	PBAT	PBAT/SiO_2 film
E. coli	–	16.7
S. aureus	–	17.2

3.8 Antimicrobial Properties

The PBAT film did not show clear microbial inhibition zones for *E. coli* and *S. aureus* (Figs. 6 and 7), reflecting no antimicrobial activity for these materials. The PBAT/SiO_2 film showed microbial inhibition zones against the two microorganisms in the disk method (Table 4). The SiO_2 nanoparticle-based films possessed good antimicrobial activity. This property will be very favorable for the applications of the novel antimicrobial packaging material. The mechanism involves the dissociation of the antimicrobial agents from the SiO_2 NPs surface and exertion of their antimicrobial effects on bacteria in suspension.

4 Conclusions

We have successfully prepared the PBAT/SiO_2 nanocomposite film via a solution casting process. Morphological, mechanical and antimicrobial activity were investigated in terms of the SiO_2 (5 wt%) content as required for packaging applications. The SiO_2 nanoparticle shows good dispersion in the PBAT matrix as confirmed by SEM. and HRTEM. TGA describes the thermal stability

of the PBAT and nanocomposite films. The mechanical strength increases by adding the SiO_2 NPs (5 wt%) into the PBAT matrix. PBAT/SiO_2 films have greater tensile strength (58.01 MPa) when compared to the PBAT polymer (33.75 MPa). PBAT/SiO_2 nanocomposite films have decreased oxygen permeability compared to the pure polymer films. The water contact angle of the obtained film was improved compared with the neat PBAT film due to the introduction of the SiO_2 NPs; the moisture uptake of the nanocomposite was decreased by adding SiO_2 NPs into the PBAT matrix. In addition, the antimicrobial activity against *S. aureus* and *E. coli* were investigated for the PBAT and PBAT/SiO_2 nanocomposite film. The PBAT/SiO_2 nanocomposite film shows excellent antimicrobial activity. Based on the results, the newly prepared nanocomposite films have improved morphological, mechanical and antimicrobial activity. Thus PBAT containing SiO_2 film may be a promising novel material for active food packaging applications.

Acknowledgments The authors thank the Department of Printing Technology, College of Engineering Guindy, Anna University, Chennai, India, for providing lab facilities and chemicals. They specially thanks the Centre for Research, Anna University, Chennai for providing funding support (Lr. No: CR/ACRF/2013/10; Dated 27.02.2013), to carry out the research work.

References

1. Calcagno CIW, Mariani CM, Teixeira SR, Mauler RS (2007) The effect of organic modifier of the clay on morphology and crystallization properties of PET nanocomposites. Polym 48:966-974
2. Hussain F, Hojjati M, Okamoto M, Gorga RE (2006) Review article: Polymer-matrix nanocomposites, Processing, Manufacturing, and application: An overview. J Compo Mate 40:1511–1575
3. Bordes P, Pollet E, Avérous L (2009) Nano-biocomposites: Biodegradable polyester/nanoclay systems. Prog Polym Sci 34:125–155
4. Sargsyan A, Tonoyan A, Davtyan S, Schick C (2007) The amount of immobilized polymer in PMMA SiO_2 nanocomposites determined from calorimetric data. Eur Polym J 43:3113–3127
5. Priestley D, Rittigstein P, Broadbelt LJ, Fukao K, Torkelson JM (2007) Evidence for the molecular-scale origin of the suppression of physical aging in confined polymer: Fluorescence and dielectric spectroscopy studies of polymer-silica nanocomposites. J Phys Cond Matt 19:205120-205132
6. Chrissafis K, Paraskevopoulos KM, Pavlidou E, Bikiaris D (2009) Thermal degradation mechanism of HDPE nanocomposites containing fumed silica nanoparticles. Thermochimica Acta 485: 65–71
7. Voronin EF, Gun'ko VM, Guzenko NV, Pakhlov EM, Nosach LV, Leboda R, Skubiszewska-Zięba J, Malysheva ML, Borysenko MV, Chuiko AA (2004) Interaction of poly (ethylene oxide) with fumed silica. J Colloid and Interf Sci 279:326–340
8. Chrissafis K, Paraskevopoulos KM, Papageorgiou GZ, Bikiaris DN (2008) Thermal and dynamic mechanical behavior of bionanocomposites: Fumed silica nanoparticles dispersed in poly(vinyl pyrrolidone), chitosan, and poly(vinyl alcohol). J Appl Polym Sci 110:1739–1749
9. Lee J, Jin Lee K, Jang J (2008) Effect of silica nanofillers on isothermal crystallization of poly (vinyl alcohol): In-situ ATR-FTIR study. Polym Test 27:360–367
10. Chung YL, Ansari S, Estevez L, Hayrapetyan S, Giannelis EP, Lai HM (2010) Preparation and properties of biodegradable starch–clay nanocomposites, vol 79, pp 391–396
11. Paul DR, Robeson LM (2008) Polymer nanotechnology: Nanocomposites. Polym 49:3187–3204
12. Glenn G, Klamczynski A, Ludvik C, Chiou BS, Shed I, Shey U, William O, Delilah W (2007) In situ lamination of starch-based baked foam packaging with degradable films. Packag Technol Sci 20:77-85
13. Shih YF, Chen RLS, Jeng J (2008) Preparation and properties of biodegradable PBS/multi-walled carbon nanotube nanocomposites. Polym 49:4602–4611
14. Kim HS, Kim HJ (2008) Enhanced hydrolysis resistance of biodegradable polymers and bio-composites. Polym Degrad Stab 93:1544–1553
15. Muthuraj R, Manjusri M, Mohanty AK (2014) Biodegradable poly (butylene succinate) and poly (butylene adipate-co-terephthalate) blends: Reactive extrusion and performance evaluation. J Polym Environ 22:336–349
16. Mohanty S, Nayak SK (2012) Biodegradable nanocomposites of poly (butylene adipate-co-terephthalate) (PBAT) and organically modified layered silicates. J Polym Environ 20:195–207
17. Venkatesan R, Rajeswari N, Thendral T (2015) Preparation and mechanical properties of Poly (butyleneadipate-co-terephthalate)-Polyvinyl alcohol/SiO_2 nanocomposite films for packaging applications. J Polym Mate 32:93–101
18. Sato M, Endo S, Araki Y, Matsuoka G, Gyobu S, Takeuchi H (2000) The flame-resistant polyester fiber: Improvement of hydrolysis resistance. J Appl Polym Sci 78: 1134–1138
19. Yoshihiro S, Yuichi S, Mitsuhiro S (2005) Nanocomposites based on poly(butylene adipate-co-terephthalate) and montmorillonite. J Appl Polym Sci 95:386–392
20. Chin-San W (2009) Antibacterial and static dissipating composites of poly (butylene adipate-co-terephthalate) and multi-walled carbon nanotubes. Carbon 47:3091–3098
21. Dajian H, Wenbo W, Yuru K, Wang Y (2012) A chitosan/poly (vinyl alcohol) nanocomposite film reinforced with natural halloysite nanotubes. Polym Compo 33:1693–1699
22. Venkatesan R, Somanathan N, Rajeswari N (2014) Structure and properties of functionalized polyfluorenone containing hetero aromatic side chains. Chin J Polym Sci 32:667–674
23. Ajith JJ, Alagar M, Thomas SP (2012) Preparation and characterization of organoclay filled polysulfone nanocomposites Mate and Manu. Pro 27:247–254
24. Venkatesan R, Rajeswari N (2015) Mechanical and antimicrobial properties of K-Carrageenan/SiO_2 nanocomposite films for active food packaging. J Polym Mate 32:457–466
25. Yang Y, Liu CH, Chang PR, Chen Y, Anderson DP, Stumborg M (2010) Properties and structural characterization of oxidized starch/PVA/α-zirconium phosphate composites. J Appl Polym Sci 115:1089–1097
26. Theapsak S, Watthanaphanit A, Rujiravanit R (2012) Preparation of Chitosan-coated polyethylene packaging films by DBD Plasma treatment. ACS Appl Mater Interfaces 4: 2744–2482